Heat and Mass Transfer 37 (2001) 321–328 © Springer-Verlag 2001

# Heat transfer during transient cooling of high temperature surface with an impinging jet

**Y. Mitsutake, M. Monde**



**Abstract** An experimental study of transient boiling heat transfer during a cooling of a hot cylindrical block with an impinging water jet has been made at atmospheric pressure. The experimental data were taken for the following conditions: a degree of subcooling of $\Delta T_{sub}$ = 20–80 K, a jet velocity of $u_j$ = 5–15 m/s, a nozzle diameter of $d_j$ = 2 mm and three materials of copper, brass and carbon steel. The block was initially and uniformly heated to about 250 °C and the transient temperatures in the block were measured at eight locations in $r$-direction at two different depths from the surface during the cooling of hot block. The surface heat flux distribution with time was evaluated using a numerical analysis of 2-D heat conduction. Behavior of the wetting front, which is extending the nucleate boiling region outward, is observed with a high-speed video camera. A position of wetting region is measured and it is correlated well with a power function of time. The changes in estimated heat flux and temperature were compared with the position of wetting region to clarify the effects of subcooling, jet velocity and thermal properties of block on the transient cooling.

**List of symbols**

| | |
|---|---|
| $a$ | proportional constant in Eq. (1) |
| $c$ | specific heat of solid |
| $D$ | diameter of heated surface |
| $d_j$ | diameter of liquid jet |
| $n$ | exponent in Eq. (1) |
| $r$ | radial coordinate |
| $r_{wet}$ | radius of trailing edge on nucleate boiling region |
| $u_j$ | jet velocity |
| $q_c$ | critical heat flux for subcooled liquid |
| $q_{co}$ | critical heat flux for saturated liquid |
| $q_w$ | wall heat flux |
| $t$ | time |
| $T$ | temperature |
| $T_b$ | block temperature |
| $z$ | axial coordinate |
| $\Delta r_b$ | width of nucleate boiling region |
| $\Delta T_{sub}$ | degree of subcooling |
| $\lambda$ | thermal conductivity of solid |
| $\rho$ | density of solid |
| $\rho_l$, $\rho_g$ | density of liquid and vapor |
| $\sigma$ | surface tension |

*Received on 17 March 2000*

Y. Mitsutake, M. Monde (✉)
Department of Mechanical Engineering
Saga University, 1 Honjo Saga City
Saga 840-8502, Japan

## 1 Introduction

A transient cooling of a hot surface with a liquid jet is commonly utilized in industrial processes or safety designs in a power plant. This heat transfer process, especially, plays an essential role in a hot rolling or a hardening on a material manufacturing process and in the emergency core cooling system during the loss of coolant accident (LOCA) in light water reactor. In these fields, many studies (Hatta et al. 1983; Carbajo 1985; Filipovic et al. 1995 and Kumagai et al. 1995) have been carried out and focused on (1) reestablishment of the wetting region, (2) the heat transfer coefficient, (3) the transient temperature distribution in and on a solid. In spite of many existing studies, it still seems that there is a problem in estimating surface temperature and heat flux accurate from the temperatures measured in the solid.

The recent progress in the project of the International Thermonuclear Experimental Reactor (ITER) needs more research for a safety analysis. Among the hypothetical accidents in a fusion reactor, an ingress of coolant accident (ICA) brings about the destruction of a vacuum vessel and the release of radio active particles contained. However, only a few studies about the ICA exist (Ogata et al. 1995; Takase et al. 1996 and Hasan et al. 1998). During the ICA, a superheated coolant liquid jet may release into a torus from a break opening on the coolant channel of the plasma facing components (PFCs). It also strikes on the very hot wall of PFCs. The flashing and heat transfer between a liquid jet and the hot wall raise a pressure in the vessel. If an excess pressurization would occur, an additional system to keep them safe should be needed. Since a flashing of jet, a pressurization of vessel, a growth of wetting region and the coexistence of different heat transfer modes on a wall are all coupled, so the transient heat transfer during the ICA becomes very complicated. The characteristics of each process must be clarified to estimate the pressurization rate and final pressure in a vacuum vessel.

The first purpose of this study is to clarify the character of surface temperature and heat flux distribution with an observation of the boiling phenomena under the atmospheric pressure prior to dealing a coupled problem on a transient cooling with the pressurization.

## 2
## Experimental apparatus and procedure

### 2.1
### Experimental apparatus

A schematic of the experimental apparatus and its main part are shown in Figs. 1 and 2, respectively. The experimental apparatus consists of three major parts: (a) heated block capsule, (b) liquid circulation system and (c) data acquisition system.



The block capsule contains the cylindrical heated block as shown in Fig. 2 the detail of which is depicted in Fig. 3. A copper, brass and carbon steel (0.45% C) are selected as the material of block to evaluate the effect of thermal properties on the transient cooling. The bottom end of cylinder serves as a heated surface facing the nozzle. The eight electrical slot heaters, 18, are mounted into the upper part of block. The cylindrical block is surrounded by the guard heater, 19, by which the radial heat loss from the peripheral wall can be reduced to provide almost adiabatic condition. Controlling slot heaters and guard heater makes temperature distribution in the block uniform. The cylindrical block is cut into two pieces along the axisymmetric surface in order to make it easy to fix thermocouples at the accurate position. After setting thermocouples at the designated positions as accurate as possible, two halves of the block are assembled to the cylinder and the clearance between them is well sealed by the soldering. Heated surface is ground into a flat surface to prevent any undulations on a surface from affecting on liquid film flow or boiling phenomenon.

Water stored in liquid tank, 2, is heated by a tank heater, 3, and then fed to nozzle, 9, by a pump, 5. The temperature of liquid jet is controlled by a cooler, 4, and a preheater, 6, equipped on a pipeline. Velocity of liquid jet is adjusted by a flow control valve, 7, up to 25 m/s.

Experiment was carried out at a velocity less than 15 m/s to ensure a stabilized circular liquid jet. During warming-up of circulating liquid, a direction of jet is changed with a rotary shutter, 20, to prevent jet from impinging on a heated surface.

### 2.2
### Data acquisition system

The data acquisition system automatically measures and records the temperatures in the block, liquid jet temperature and pressure drop at the nozzle.

As shown in Fig. 3, the temperatures are measured at every eight radial positions on the planes of 1 and 5 mm

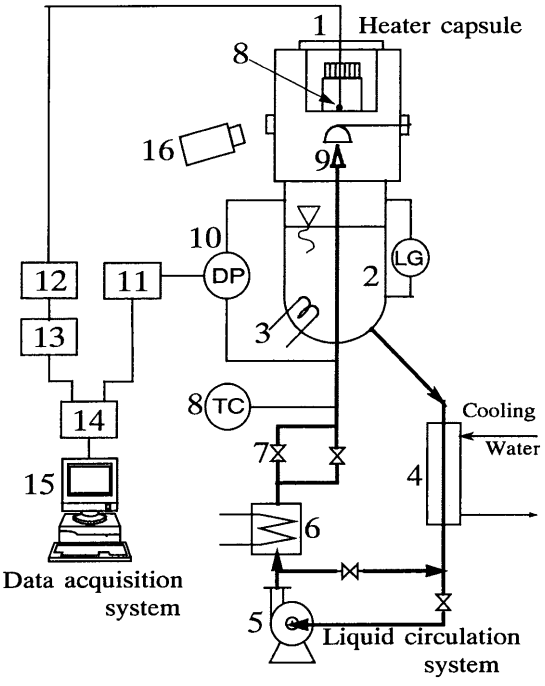


**Fig. 1.** Whole of experimental apparatus. 1: Block capsule; 2: liquid tank; 3: tank heater; 4: cooler jacket; 5: pump; 6: preheater; 7: flow control valve; 8: thermocouple; 9: nozzle; 10: differential pressure transducer; 11: dynamic strain meter; 12: ice box; 13: voltage amplifier; 14: A/D converter; 15: computer; 16: high speed video camera

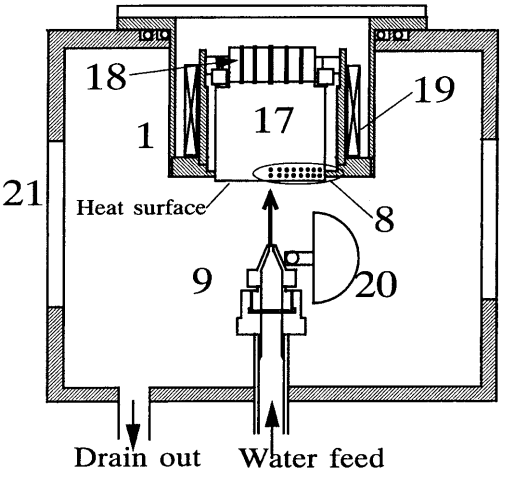


**Fig. 2.** Main part of experimental apparatus. 17: Cylindrical block; 18: slot heaters; 19: guard heater; 20: rotary shutter; 21: window

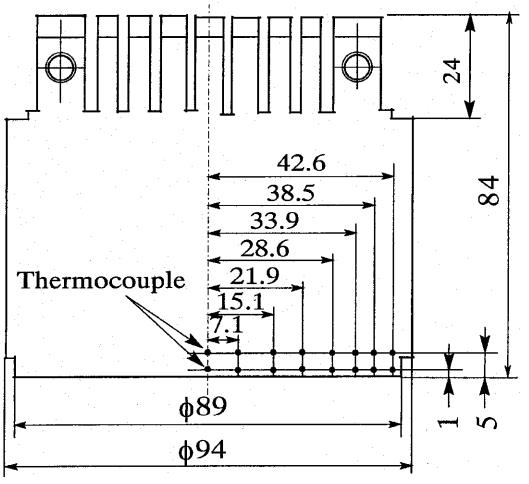


**Fig. 3.** Schematic of the cylindrical heated block

below the heated surface with a K-type thermocouple of 0.1 mm in diameter. An icebox, 12, is used as a reference point. Very low voltage signal of thermocouple is amplified by a voltage amplifier, 13, and it is directly sampled by a computer, 15, with analog/digital converter, 14. The temperature changes at 16 points are simultaneously sampled with 500 Hz and these can be stored up to about 200 s. The pressure drop at the nozzle is measured by a differential pressure transducer, 10, and a dynamic strain meter, 11, to evaluate the jet velocity. The jet velocity is calculated from the pressure drop and the flow coefficient of the nozzle calibrated previously. A noise included in the data sampled is reduced with the Savitzky–Golay method.

### 2.3
### Experimental procedure and uncertainty analysis

The combinations of the experimental conditions are tabulated in Table 1. The heated surface is polished with Emery paper (#800) to maintain the same surface condition before every experimental run. In order to insure the axisymmetry of cooling, one carefully adjusts the position of block capsule until the center of heated surface meets with the stagnant of jet. The transient cooling is also observed with high speed video camera, 16, at a frame rate up to 2000 frames/s.

Results of uncertainty analysis for the measurements such as jet velocity, temperatures and positions of thermocouple are tabulated in Table 2.

## 3
## Results and discussions

### 3.1
### Observation of boiling phenomena

From observation of the flow aspect on the surface, the process of transient cooling can be divided into three following regions; non-wetting region, spreading of wetting region and fully wetted region.

In the non-wetting region, the heated surface is hardly wetted in a short time immediately after the jet impingement because the liquid jet is completely splashed out as small droplets. It appears that a stable solid–liquid contact does not establish even in the stagnant point. The time during which the surface is not wetted, becomes longer for the material of larger thermal inertia, $(\rho c\lambda)^{1/2}$, which may govern the interface temperature at the solid–liquid contact.

**Table 2.** Uncertainty in measurements

| Quantity | Relative/total uncertainty |
|---|---|
| Jet velocity $u_j$ | $\delta u_j/u_j = \pm 4.6\%$ |
| Temperature | $\delta T = \pm 0.8$ °C at 250 °C |
| Position $r_i$, $z_j$ | $\delta r$, $\delta z = \pm 0.1$ mm |

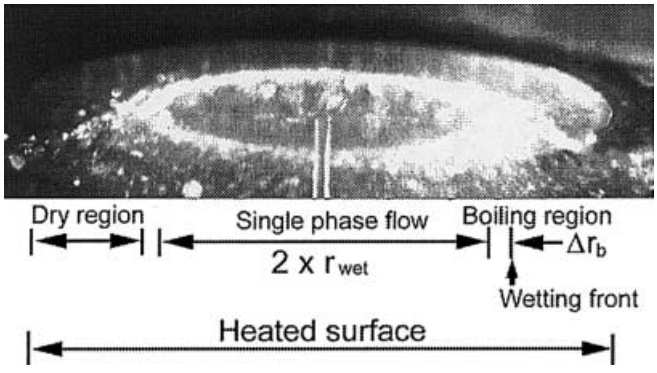


**Fig. 4.** Photograph of flow boiling ($u_j$ = 5 m/s, $\Delta T_{sub}$ = 80 K, Brass, $t$ = 12 s after impingement)

After a short time of the jet impingement, solid–liquid contact was first reestablished at the stagnant point of jet. As time is passing, the wetting region is spreading from the center to the circumference of the heated surface as shown in Fig. 4. In this situation, three major heat transfer regions coexist on the heated surface; (a) single-phase forced heat transfer region, (b) nucleate boiling region and (c) dry region from the center, respectively. An annular shape of the width of $\Delta r_b$ looks like white due to the occurrence of violent nucleate boiling and then appears to be limited in the area close to the solid–liquid contact line, beyond which the radial liquid film flow is completely splashed as droplets by the violent boiling. Therefore, non-wetted area still exists on the surface beyond the solid–liquid contact line. The value of width, $\Delta r_b$ is hardly

**Table 1.** Experimental range

| | | | |
|---|---|---|---|
| Coolant | Water | | |
| Pressure | 0.1 MPa | | |
| Initial block temperature | 250 °C | | |
| Nozzle diameter $d_j$ | 2 mm | | |
| Jet velocity $u_j$ | 5, 10, 15 m/s | | |
| Reynolds number of jet $Re_j$ | $10^4$–$3 \times 10^4$ | | |
| Subcooling of jet $\Delta T_{sub}$ | 20, 50, 80 K | | |
| Block material | Copper | Brass (70 Cu, 30 Zn) | Carbon steel (0.45 C) |
| Thermal property of block at 250 °C | | | |
| $\rho$ [kg/m$^3$] | 8805.6 | 8530.0 | 7783.1 |
| $c$ [kJ/kg/K] | 0.411 | 0.4298 | 0.539 |
| $\lambda$ [W/m/K] | 381.8 | 112.2 | 37.76 |
| $a \times 10^4$ [m$^2$/s] | 1.055 | 0.306 | 0.0900 |
| $\sqrt{\rho c\lambda} \times 10^{-3}$ [W$\sqrt{s}$/(m$^2$K)] | 37.28 | 20.06 | 12.59 |
| $\lambda/\sqrt{\rho c} \times 10^3$ [$\sqrt{\text{Wm}/(\text{sK})}$] | 200.2 | 58.7 | 18.44 |

changed during cooling and it seems to be affected only by the degree of subcooling and the material of block. As the degree of subcooling increases from $\Delta T_{sub}$ = 20–80 K, the value of $\Delta r_b$ approximately decreases from 4 to 2 mm for the brass and the carbon steel, while from 15 to 7 mm for the copper. The reason why the value of $\Delta r_b$ decreases with an increase in the subcooling and the value of $(\rho c\lambda)^{1/2}$, may be governed by combination between heat removed by the cooling of liquid film and heat transferred by heat conduction in the solid. On other words, an enhancement in the cooling by the liquid film reduces the boiling area due to a shortage of heat conducted through the solid side, while for a constant cooling rate by the liquid film, an increase in the value of $(\rho c\lambda)^{1/2}$, supplies heat enough to enlarge the boiling area. After the wetting front reaches the end of the heated surface, it is cooled only with a single-phase liquid film flow and then major transient cooling is finished.



Above observation, finally, tells us that most effective cooling was made by nucleate boiling limited in a narrow annular region and then the nucleate boiling region moves in *r*-direction with time. The growth of wetting region has a significant effect on a distribution of transfer heat rate.

### 3.2
### Growth of wetting region with time

It is found that the position at which the wetting front moves with time is very important to predict the amount of heat removed from the hot surface. However, the position of the wetting front was rather indistinct due to a blockage of the droplets as shown in Fig. 4. Instead of the wetting front on which boiling starts being generated, therefore, the radial position, $r_{wet}$, of the trail edge in nucleate boiling region can be measured easier. This position can be defined as the boundary between the single-phase liquid film flow and the nucleate boiling regions and its boundary is found to be clearly identified with ±1 mm uncertainty.

Figure 5 shows, for an example, the change of the position, $r_{wet}$, for $u_j$ = 5, 10, and 15 m/s and $\Delta T_{sub}$ = 50 K plotted against time after the jet impingement. In order to approximate each curve for the position, one may assume a tentative function of the position, $r_{wet}$, as the power function with respect to time as given by Eq. (1) and then determine the values of the constant, *a*, and the exponent, *n*, using least mean square method.

$$r_{wet} = a \cdot t^n \qquad (1)$$

The values of *a* and *n* determined thereby are plotted against the jet velocity, $u_j$ or the subcooling, $\Delta T_{sub}$, as shown in Figs. 6–8. Each curve in Fig. 5 is depicted by using the values of *a* and *n* determined.

Agreement between the estimated curve and data is found to be good at most of the experimental conditions except for the case of copper, $u_j$ = 5 m/s and $\Delta T_{sub}$ = 20 K for which the wetting region hardly grows. The experimental data reveal from Fig. 5 that the wetting region spreads faster with increasing the jet velocity and also subcooling and according as the steel, the brass and the copper of which corresponds where the order just corresponds to that of the value of thermal inertia $(\rho c\lambda)^{1/2}$. The result may come from a balance between the cooling rate by the liquid film and the heat conducted through the hot block.

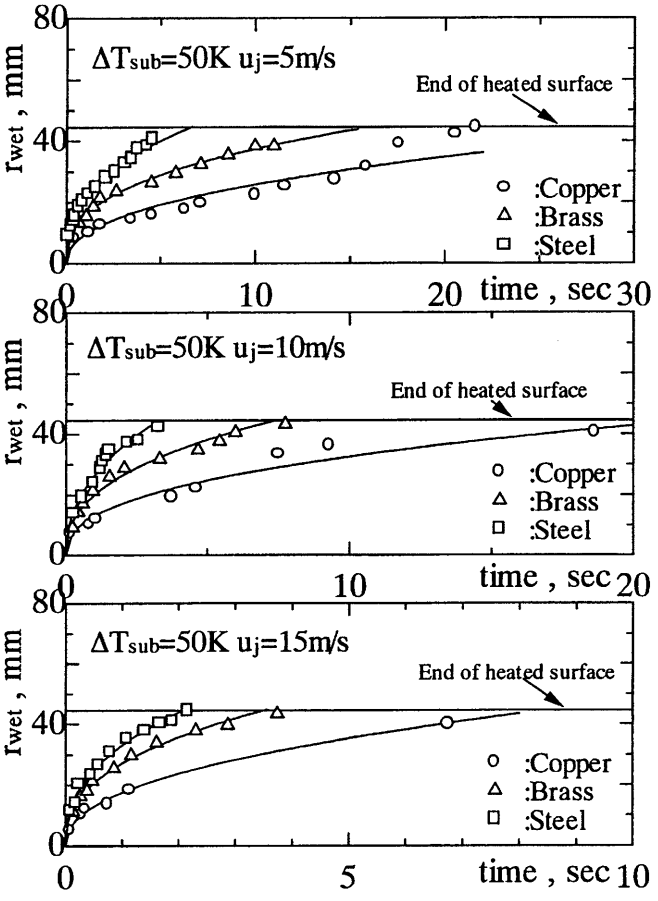


**Fig. 5.** Radius of the trail edge of nucleate boiling region for $\Delta T_{sub}$ = 50 K

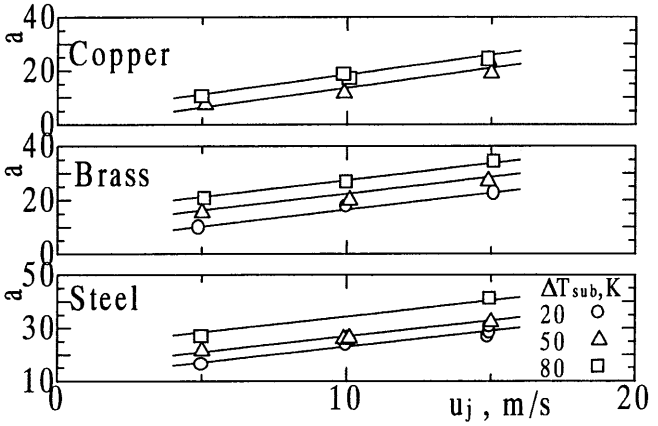


**Fig. 6.** The relationship between constant *a* and jet velocity, $u_j$

Figures 6–8 show the effect of jet velocity $u_j$ and subcooling $\Delta T_{sub}$ on the constant, *a* and the exponent, *n* in Eq. (1). In these figures, each line is drawn to show the trend in the values of *a* and *n*. The value of *a* in Figs. 6 and 7 has a dimension being measured for the position of $r_{wet}$ in mm and time of *t* in sec.

Figures 6 and 7 reveal that the constant $a$ can be expressed by the linear function of jet velocity $u_j$ and degree of subcooling $\Delta T_{sub}$. Slopes of the linear relationships in these figures take a fixed value depending on a material and these are tabulated in Table 3. For the fixed values of $u_j$ and $\Delta T_{sub}$, the constant, $a$, takes a larger value according as the carbon steel, the brass and the copper.

Figure 8 shows that the exponent, $n$, appears to be independent of the jet velocity and thermal property of the block, while it weakly depends on the subcooling $\Delta T_{sub}$ and the slope of the line in Fig. 8 is very small value of $-1.90 \times 10^{-3}$ [1/K]. The exponent of $n$ changes from 0.4 to 0.5 over the range from $\Delta T_{sub}$ = 20–80 K. Hatta et al. (1983) reported that the progress of the wetting region was given by $r_{wet} = a\, t^{1/2}$ for a stainless steel plate under the experimental condition; $u_j$ = 2.0 and 3.4 m/s, $\Delta T_{sub}$ = 80 K, and initial temperature of 900 °C. It may be of worth mentioning that both exponents almost coincide.

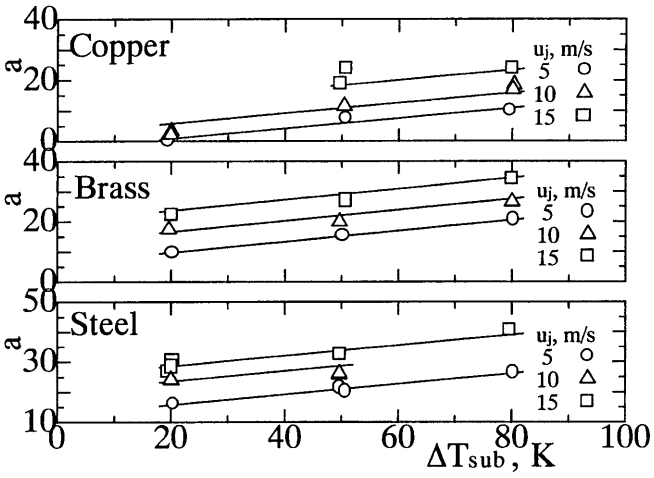


**Fig. 7.** Relationship between constant $a$ and subcooling, $\Delta T_{sub}$

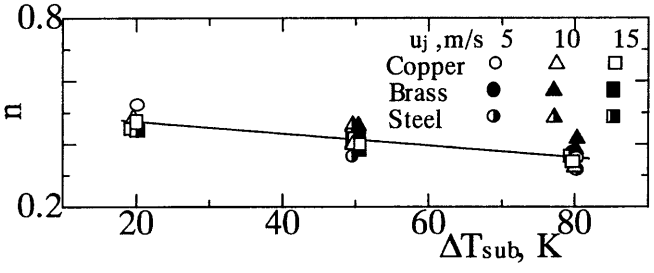


**Fig. 8.** Relationship between exponent $n$ and subcooling, $\Delta T_{sub}$

**Table 3.** Slopes of linear relationships between $a$ and $u_j$, $\Delta T_{sub}$

| Material | Slope of $a$ in | |
|---|---|---|
| | Fig. 6 | Fig. 7 |
| Copper | 1.46 | 0.168 |
| Brass | 1.18 | 0.182 |
| Carbon steel | 1.08 | 0.176 |

### 3.3
### Variation of surface temperature

The temperatures discretely measured at the 8 positions in $r$-direction on the planes of two different depths, are used to interpolate continuous radial temperature distribution with a 3rd order Spline function.

The radial temperature distributions at depth of 1 mm for $u_j$ = 5 m/s, $\Delta T_{sub}$ = 50 K for three materials are shown in Fig. 9. A thin curve on the $t$-$r$ plane in Fig. 9, for reference, denotes the position of the trailing edge, $r_{wet}$, with time and then a thick curve on the temperature surface is locus of temperature at $r = r_{wet}(t)$. According to observation of flow aspect on the surface, the width of the nucleate boiling, $\Delta r_b$, is found to depend on thermal properties of the block, the jet velocity and subcooling. In the case of $u_j$ = 5 m/s and $\Delta T_{sub}$ = 50 K, the values of $\Delta r_b$ becomes about 7, 3 or 3 mm depending on whether the block material is the copper, the brass or the carbon steel. Superposition of $\Delta r_b$ on the line for the trailing edge gives the position of the wetting front. As the result, one can know where the nucleate boiling area exists and moves outward with time as shown by a shadow area in Fig. 9. It may be necessary to mention that a time lag exists in the origin of time between the measurement of the temperature and the position of the trailing edge, because it takes a short time for impinging jet to make the hot surface wet as already explained in Sect. 3.1 and both measurements do not synchronize. It should be hoped to make the time lag clear. There is another time delay between the surface temperature estimated and the temperature measured on the plane of 1 mm in depth. To evaluate this time delay, one may apply the solution of semi-infinite 1-D heat conduction showing that even for the carbon steel being the poorest thermal conductivity, it is less than 0.01 s. Consequently, the time delay can be considered to be negligible small so that the temperature measured at 1 mm in depth can be approximately considered as the surface one.

Figure 9 shows that for the case of the carbon steel the sudden drop in temperature almost starts at around time when the wetting front reaches, while for the cases of the copper and the brass the gradual decrease in the temperature seems to start before the wetting front reaches. On comparison of temperature drop and the position of the shadow area, in the case of the copper much heat would be transferred by the heat conduction in $z$- and $r$-directions. In addition, we notice that as the wetting region spreads faster or the thermal conductivity becomes larger, the radial heat conduction becomes important as compared with axial one, namely the nature of 2-D heat conduction in the block comes out strongly.

### 3.4
### Estimation of surface heat flux

Another important parameter is surface heat flux to evaluate heat transfer rate by impinging jet. In order to calculate surface heat flux, $q_w$, one may employ the discretized 2-D energy balance equations as given in Eq. (2) and a domain for calculation as given by the layer of 2 mm in depth from the surface as shown in Fig. 10. Heat flux between the cells is calculated from Eq. (3) with the measured temperatures at two different depths.

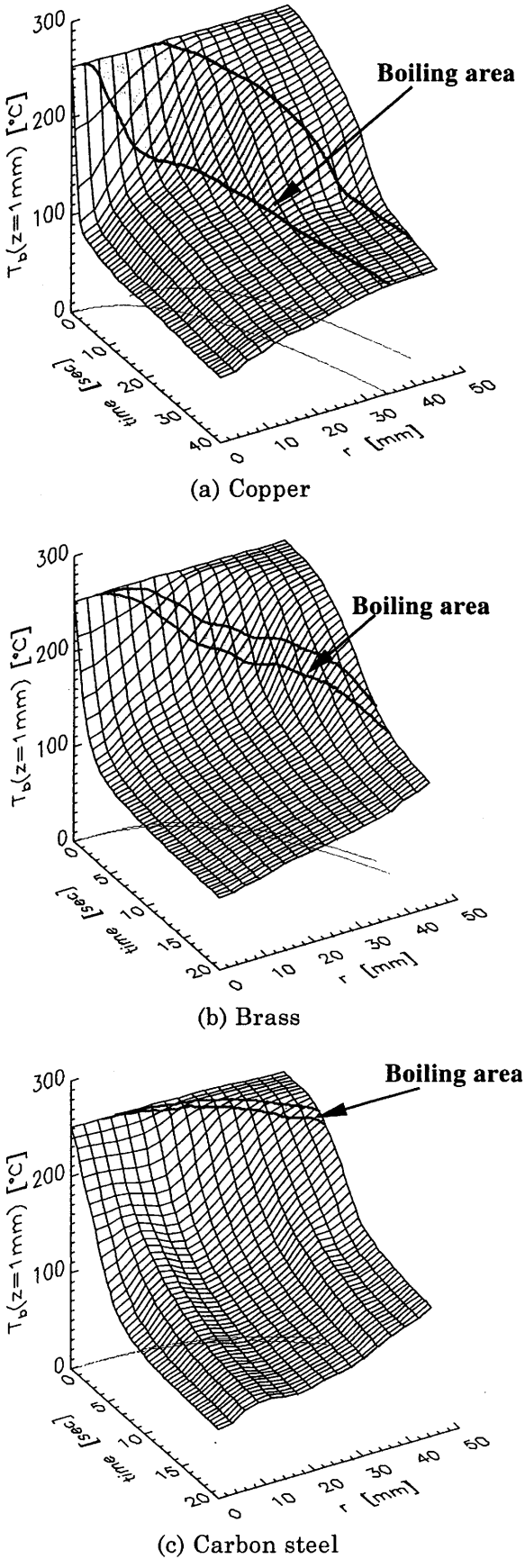


**Fig. 9a–c.** Comparison of radial temperature distribution and wetting region under the condition: $z$ = 1 mm, $u_j$ = 5 m/s, $\Delta T_{sub}$ = 50 K

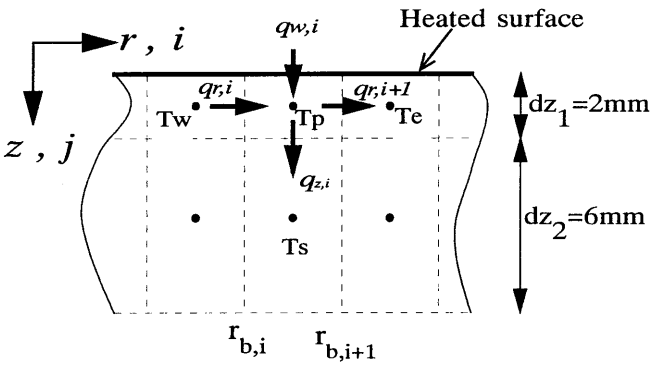


**Fig. 10.** A schematic of heat flow between control volumes

$$c_p\rho(\pi(r_{b,i+1}^2 - r_{b,i}^2)\Delta z_1)\frac{dT_{i,1}}{dt} = 2\pi r_{b,i}q_{r,i}\Delta z_1 - 2\pi r_{b,i+1}q_{r,i+1}\Delta z_1 + \pi(r_{b,i+1}^2 - r_{b,i}^2)(q_{w,i} - q_{z,i}) \quad (2)$$

$$q_{r,i-1} = -\lambda\frac{T_{i,1} - T_{i-1,1}}{r_i - r_{i-1}}, \quad q_{r,i} = -\lambda\frac{T_{i,2} - T_{i,1}}{r_{i+1} - r_i},$$

$$q_{z,i} = -\lambda\frac{T_{i,2} - T_{i,1}}{z_2 - z_1} \quad (3)$$

A mesh number of 74 in $r$-direction and a time step of 10 ms are enough for the solution to converge. The radial temperature distributions are interpolated by a 3rd order Spline function with the measured temperature. An accuracy of the estimated heat flux with Eq. (2) is simply checked by using the exact solution of 1-D heat conduction where a constant heat flux is added to a heated surface. For the copper block, the response time of 1.5 s is needed until an estimated heat flux agrees with an actual heat flux. For the case of brass and carbon steel, the response time of 3.8 and 9.9 s are needed, respectively.

The estimated heat flux at a steady state becomes 98.6, 97.2 and 95.3% of the added heat flux for copper, brass and carbon steel, respectively. These errors may arise from the delay of temperature propagation between the heated surface and the measured point or from the use of first order derivative formula.

### 3.5 Radial heat flux distribution

Figure 11 shows the variation of the radial heat flux against time for three different materials. The thin curve on the $r$-$t$ plane, the thick curve on the heat flux surface and a shadow area in Fig. 11 are the same as those in Fig. 9. It should be noted here that discussing when the peak heat flux arises compared with the shadow area, we always have to take into account the response time in a heat flux measurement as mentioned previously. From these figures it is found that the peak heat flux is initially attained at $r$ = 0 and it moves outward decreasing in its value with time. A peak heat flux at $r$ = 0 reaches up to about 16.6, 3.4 and 1.9 MW/m$^2$ for the copper, the brass, the carbon steel, respectively. The locus of the peak heat flux looks like a ridge. From the comparison of the ridge with the shadow area, the maximum heat flux at a certain position seems to occur after passing of the nucleate region

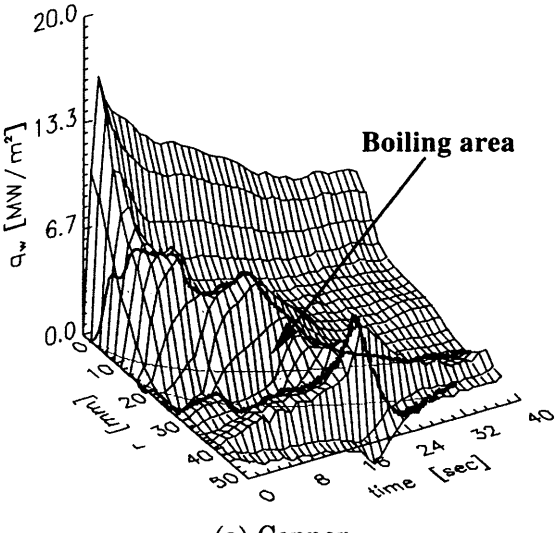


(a) Copper

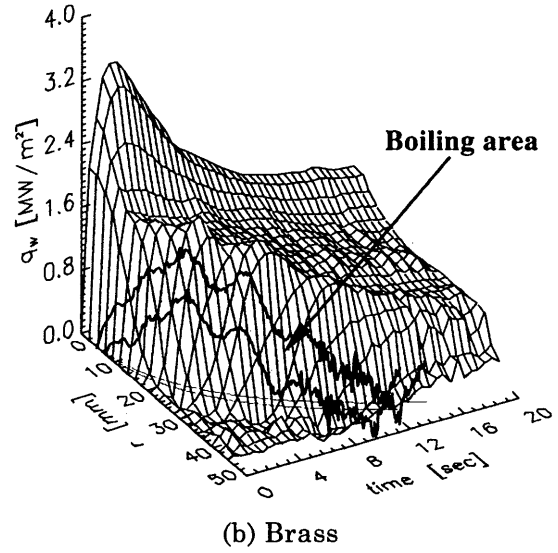


(b) Brass

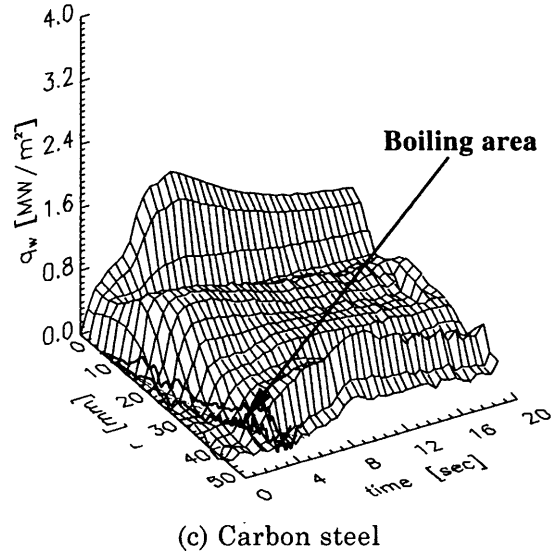


(c) Carbon steel

**Fig. 11a–c.** Change in radial heat flux distribution and locus of trailing edge position of wetting region under the experimental condition: $u_j$ = 5 m/s, $\Delta T_{sub}$ = 50 K

and the disagreement becomes larger for the carbon steel and the brass due to a larger time lag. When the ridge of the heat flux surface is shifted as an estimated response time in the direction of $t$ axis, maximum heat flux on a certain position would take place when the nucleate boiling covers there. The above trend in the heat flux distribution is the same for the other experimental conditions.

## 4
## Comparison of transient maximum heat flux and steady critical heat flux



Monde et al. (1994) proposed a generalized correlation to predict critical heat flux in a forced convective boiling with an impinging jet as:

$$\frac{q_c}{q_{co}} = \frac{1+\sqrt{1+4CJa}}{2} \tag{4}$$

where

$$\frac{q_{co}}{\rho_v H_{lg} u_j} = 0.221\left(\frac{\rho_l}{\rho_g}\right)^{0.645}\left(\frac{2\sigma}{\rho_l u^2 (D-d_j)}\right)^{0.343} \times (1+D/d_j)^{-0.364}$$

$$C = \frac{0.95(d/D)^2(1+D/d_j)^{-0.364}}{(\rho_l/\rho_g)^{0.43}(2\sigma/\rho_l u_j^2(D-d_j))^{0.343}}$$

Figure 12 show a comparison between transient maximum heat flux and critical heat flux predicted by Eq. (4) in which the diameter of $D$ may be tentatively replaced by $D = 2r_{wet}$, although it is not yet clear, exactly speaking, whether the transient maximum heat flux occurs just at the wetting front or not.

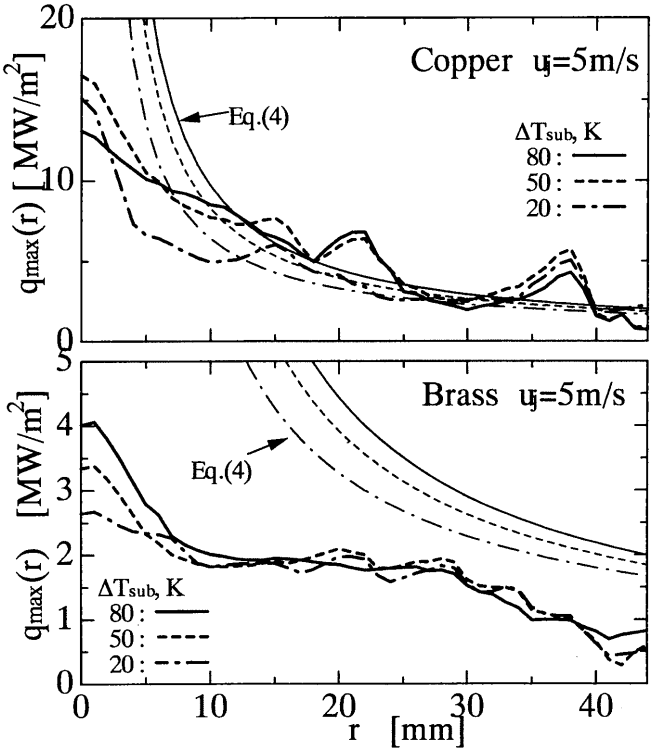


**Fig. 12.** Comparison between transient maximum heat flux and critical heat flux

In Fig. 12, as a representative case, the data for $u_j$ = 5 m/s are chosen. It seems from Fig. 12 that for the copper block, both values interestingly agree except for the region being smaller than $r$ = 10 mm and unknown irregularity of the heat flux at a position, while for the brass block, the heat flux at steady state becomes larger than one at transient state. The reason that the difference between transient and steady heat fluxes becomes larger for the brass block than that for the copper block may be attributed to a deficiency of heat transferred by heat conduction in the solid. The reason that in the copper block within the region of $r \leq 10$ mm, the difference between transient and steady heat fluxes becomes significantly large compared with the other region of $r \geq 10$ mm, may be attributed to the same fact. In other words, if the heat conduction in the solid supplies heat enough, then the transient heat flux may approach close to steady heat flux predicted by Eq. (4).



## 5 Conclusions

1. The radius of the advancing trailing edge of annular nucleate boiling region $r_{wet}$ was measured as concerning with the wetting front.
2. The radius of the advancing trailing edge of annular nucleate boiling region $r_{wet}$ is correlated well by the power function of time given by Eq. (1). The effect of sub-cooling, jet velocity and material on the parameters governed Eq. (1) was obtained.
3. The peak heat flux at a certain radial position seems to occurs where nucleate boiling region occurs.

## References

**Carbajo JJ** (1985) A study on the rewetting temperature. Nuclear Eng Des 84: 21

**Filipovic J; Incropera FP; Viskanta R** (1995) Quenching phenomena associated with a water wall jet: I. Transient hydrodynamic and thermal conditions. Experimental Heat Transfer 8: 97

**Hasan MZ; Monde M; Mitsutake Y; Iwamoto K** (1998) An experimental study of ingress-of-coolant accident in fusion reactors. Fus Eng Des 42: 73

**Hatta N; Kokado J; Hanasaki K** (1983) Numerical analysis of cooling characteristics for water bar. Transactions of the Iron and Steel Institute of Japan 23: 555

**Kumagai S; Suzuki S; Sano Y; Kawazoe M** (1995) Transient cooling of a hot metal slab by an impinging jet with boiling heat transfer. ASME/JSME Thermal Eng. Joint Conf., Fletcher, L. S. and Aihara, T., 2: 347, ASME, New York

**Monde M; Kitajima K; Inoue T; Mitsutake Y** (1994) Critical heat flux in a forced convective subcooled boiling with an impinging jet. Heat Transfer 7: 515–520

**Ogawa M; Kunugi T** (1995) Thermohydraulic experiments on a water jet into vacuum during ingress of coolant event in a fusion experimental reactor. Fus Eng Des 29: 233

**Takase K; Kunugi T; Seki Y; Kurihara R; Ueda S** (1996) A fundamental study of a water jet injected into a vacuum vessel of fusion reactor under the ingress of coolant event. Fus Tech 30: 1453